SKI Report 95:29

SITE-94

Some Properties of Copper and Selected Heavy Metal Sulfides

A Limited Literature Review

Hans-Peter Hermansson

June 1995

ISSN 1104-1374
ISRN SKI-R--95/29--SE

SKI
STATENS KÄRNKRAFTINSPEKTION
Swedish Nuclear Power Inspectorate

SKI Report 95:29

SITE-94

Some Properties of Copper and Selected Heavy Metal Sulfides

A Limited Literature Review

Hans-Peter Hermansson

Studsvik Material AB, 611 82 Nyköping, Sweden

June 1995

PREFACE

This report concerns a study which is part of the SKI performance assessment project SITE-94. SITE-94 is a performance assessment of a hypothetical repository at a real site. The main objective of the project is to determine how site specific data should be assimilated into the performance assessment process and to evaluate how uncertainties inherent in site characterization will influence performance assessment results. Other important elements of SITE-94 are the development of a practical and defensible methodology for defining, constructing and analyzing scenarios, the development of approaches for treatment of uncertainties, evaluation of canister integrity, and the development and application of an appropriate Quality Assurance plan for Performance Assessments.

Johan Andersson
Project Manager

Some properties of copper and selected heavy metal sulfides. A limited literature review

Hans-Peter Hermansson
Studsvik Material AB, 611 82 NYKÖPING

Abstract

The Swedish nuclear inspectorate will review the concept of a future high level nuclear waste storage which SKB is going to issue. Therefore it is necessary for the inspectorate to collect various types of knowledge to be able to review the SKB proposal. One part of the storage system will be the copper container. The chemical and physical behavior of copper in the repository environment will therefore be of critical importance for the repository integrity. The present work concerns a literature review of copper and selected heavy metal sulfides as they are expected to play an important role at copper corrosion in the repository environment. The interest is focused on their properties as described by crystal structure, electrical properties, atom mobility, solubility in water, mechanisms of sulphidation and selected thermodynamical data.

Various types of information on sulfide phases and their formation have been found. There are results from studies in gaseous as well as in solution environment. Some important observations are summarized at the end of the main chapters of "Sulfide phases and their formation", "Diffusion and diffusion routes", "Solubility" and "Thermodynamics".

Contents

		Page
1	**Introduction**	**1**
2	**Sulfide phases and their formation**	**2**
2.1	Tarnishing and atmospheric corrosion	2
2.2	Processes in solution	8
2.3	Structures and phase relations	10
2.4	Microbially induced corrosion	12
2.5	Some important observations	13
3	**Diffusion and diffusion routes**	**14**
3.1	General	14
3.2	Some important observations	19
4	**Solubility**	**21**
4.1	General	21
4.2	Some important observations	24
5	**Thermodynamics**	**25**
5.1	Data	25
5.2	Phase diagrams	27
5.3	Some important observations	29
6	**Structure**	**30**
7	**Leaching**	**31**
8	**Kinetics**	**32**
9	**Conductivity**	**33**
10	**Pitting corrosion**	**34**
11	**Other heavy metals**	**35**
References		**36**

Executive summary

The present work concerns a literature review of copper and selected heavy metal sulfides as they are expected to play an important role at copper corrosion in the repository environment. The interest is focused on their properties as described by crystal structure, electrical properties, atom mobility, solubility in water, mechanisms of sulphidation and selected thermodynamical data.

In works related to tarnishing and atmospheric corrosion of copper, activation energies of 63 kJ/mol and 38 kJ/mol have been found, reflecting reaction mechanisms initially controlled by interface reactions and in later stages by diffusion through or in a Cu_2S layer. At tarnishing of a Au-Ag-Cu alloy, the layer formation followed linear kinetics at formation of Ag_2S, CuS and Cu_2S. The formation of silver and copper sulfides has been found to be promoted by the presence of air pollution species as $NO_2(g)$ and $Cl_2(g)$. This demonstrates the importance to know the full influence on copper corrosion of all material present in a repository environment. It has also been demonstrated that already a few monolayers of adsorbed water with dissolved gases are sufficient to initiate electrochemical corrosion processes on the surface of metals in electrical contacts (silver, copper and gold).

The photodoping process in a thin-film, light-sensitive structure has shown that the influence of irradiation on silver and copper sulfide nucleation, formation and the resulting transportation properties, are important and should consequently be considered for the repository environment.

At high temperature it was found that sulfidation follows a parabolic rate law with different activation energies in the low- and high-temperature ranges. Parabolic rate constants of sulfidation were used to calculate average self-diffusion coefficients of copper in Cu_2S and their temperature dependence.

It has been demonstrated that the formation of silver sulfide in aqueous systems is easy also in the presence of strong complexing agents. EDTA will, however, inhibit CuS precipitation but only for periods of a few hours. This demonstrates the large driving force for silver and copper sulfide formation. It should also be pointed out that bisulfide competes with the chelators for surface sites on the sulfide phase. The rate law suggests that, in case of copper, growth is controlled by encounters between HS- bound to the surface and chelated copper from the solution. Growth is diffusion limited.

Low chalcocite is found to be monoclinic and contains 48 Cu_2S units per cell. The structure is based on a hexagonal-close-packed framework of sulfur atoms, with copper atoms occupying mainly triangular interstices. Djurleite is also monoclinic. The structure is similar to the low chalcocite structure. The phase state of the Cu_2S--FeO system was investigated at temperatures up to 1450 °C and gas phase oxygen partial pressures in the range 10^{-1} - 10^{-7} Pa. Phase equilibria of the copper-sulfur system were investigated from 0° to 250°C over the composition range Cu/S = 0.95-2.10. The two blaubleibender covellites,

low digenite, a nameless tetragonal phase and protodjurleite were found to be metastable. The proposed $Cu_{1.9}S$ phase was demonstrated not to be a real phase in the system.

The drift pathway of copper ions was discussed from population data of the copper suifides and the temperature dependence of diffusion coefficients was determined.

The measurements on the low temperature phase of Cu_2S give chemical diffusion coefficients ranging between $6*10^{-6}$ cm^2 /s and $1*10^{-7}$ cm^2/s at 60°C.

Chemical diffusion coefficients have been measured at 20 °C. For chalcocite (Cu_2S) they range between $1*10^{-6}$ and $1.3*10^{-8}$ cm^2/s, and for β-Cu_2Se between $2.4*10^{-6}$ and $4.3*10^{-7}$ cm^2/s, whereas djurleite ($Cu_{1.95}S$) shows only slightly varying values between $1.4*10^{-8}$ and $2.4*10^{-8}$ cm^2 /s. Drift pathways of copper ions were discussed from population data.

The copper ions partially occupy two sets of three-coordinated sites within the HCP sulfur array and display anharmonic thermal motion. The results suggest that the conductivity is two dimensional in nature. Copper ions are distributed to the tetrahedral, trigonal and octahedral interstitials of the chalcogen atoms. The distribution of the copper ions was studied as a function of temperature. The diffusion path of the mobile copper ions was also discussed.

The effect of copper diffusion from the p-Cu_2S into the n-CdS region, due to heat treatment, in a Cu_2S/CdS heterojunction photovoltaic cell was investigated. Diffusion coefficients in the midgrain and grain boundary regions were evaluated for Cu_2S. In the chemiplating process copper diffusion is $5*10^2$ times faster in the grain boundary than in midgrain. Analysis yields diffusion coefficients of $5.8*10^{-11}\exp(-0.229/kT)$ in midgrain and $1.06\exp(-0.964/kT)$ in the grain boundary.

Because polysulfide complexes are extremely stable, the solubility of copper in sulfidic waters is strongly dependent on the activity of solid sulfur, a_S^0.

The solubility of Ag_2S (acanthite/argentite) was measured in vapor saturated aqueous sulfide solutions at 25-300 °C, total sulfide = 0.2 - 1.4 M, and pH_{25} = 5.8 - 7.3. Under these conditions, Ag_2S was found to dissolve under formation of $Ag(HS)_2^-$ which appears to be the dominant silver species in this type of hydrothermal fluids.

The equilibrium constant at 25 °C for the following reaction has been measured in NaCl media:

$$CuS(cov) + H^+(aq) = Cu^{2+}(aq) + HS^-(aq),$$

Where CuS(cov) designates synthetic covellite. Values of pK_{sp} are 21.39, 21.04, and 20.95 at [NaCl] = 0.2, 0.7, and 1.0 M, respectively.

Potential pH-diagrams (Pourbaix diagrams) for the Cu - H_2O, Fe - H_2O and Fe - Cu - H_2O systems are presented and the solubilities of copper and iron oxides (including mixed copper-iron oxide) are evaluated. Thermochemical data are used to construct a modified log-activity diagram for the system Cu-H-O-Cl-(CO_2). Heat capacities of $Cu_{1.90}S$, $Cu_{1.95}S$, $Cu_{1.98}S$ and $Cu_{1.995}S$ are accounted and a revised version or the copper-rich part or the phase diagram is presented. Heat capacities of $Cu_{1.75}S$, $Cu_{1.80}S$, and $Cu_{1.85}S$ have been measured by adiabatic-shield calorimetry from 5 to about 700 K. The heat-capacity curves show transitions near 312, 337, and 355 K in $Cu_{1.75}S$ and $Cu_{1.80}S$ and near 312, 368, and 376 K in $Cu_{1.85}S$, which implies revision of existing phase diagrams.

The copper-sulfur phase diagram has been drawn from 20 °C to 500 °C, in the compositional region $Cu_{2.000}S$-$Cu_{1.96}S$.

X-ray diffraction data collected on a single crystal specimen of CuS_2 show that despite its optical anisotropy CuS_2 apparently has the cubic pyrite structure, with a = 5.7891(6)A. The CuS_6 octahedron is only slightly distorted, which is in contrast with the square-planar coordination usually found for Cu^{2+}.

The system CuAgS was also investigated. This system is characterized by several phases with highly disordered cation sites, extensive solid solutions, and solid reaction rates so rapid as to be unquenchable.

The Ag_3CuS_2 structure is based on distorted bcc packing of sulfur. There are two distinct silver sites. In one of them the silver atom is surrounded by six sulfur atoms forming a [2+4] distorted octahedral environment. In the other site the silver atom is in a distorted tetrahedral environment with two sulfur atoms nearby and two more, somewhat farther away. Copper is linearly coordinated by two sulfur atoms.

It is shown that the overall sulfide induced pitting process on copper can be described by the following three stages. The first stage corresponds to the nucleation and growth of a complex copper sulfide layer at potential values close to the equilibrium potentials of the Cu/Cu_2S and Cu/CuS reversible electrodes. The second stage is related to the rupture of the copper sulfide film at potentials more positive than a certain critical value, leading to pitting corrosion of copper metal and yielding a poorly protective copper sulfide layer. The third stage occurs in the copper oxide electroformation range, where the presence of copper sulfide accelerates the electrodissolution of the base metal and copper oxide hinders the sulfidization processes. The current transients of each stage are interpreted through a model based on the nucleation and growth mechanism.

From archaeological finds it has been observed that grain size and shape is the factor governing the corrosion durability of lead. For long term corrosion stability, the grain size should not exceed 0.5 mm grain diameter. Copper and copper-iron sulfides can be classified into three general groups: (1) anilite,

digenite, geerite, cubanite, chalcopyrite, haycockite, talnakhite, mooihoekite and bornite with structures based upon approximate cubic closepacking of the sulfur atoms; (2) djurleite and chalcocite with structures based upon approximate hexagonal closepacking of the sulfur atoms; (3) covelline, yarrowite, spionkopite and idaite with a combination of hexagonal close packing and covalent bonding of the sulfur atoms. Nothing has earlier been published on fusion in the Cu_2S-$FeSNa_2S$-PbS system; only the binary and ternary system which form the edges and faces of the concentration tetrahedron of this quaternary system have been studied and their equilibrium diagrams constructed. The composition found for the copper rich double compound in the Cu_2S-Na_2S system by Kopylov and Novoselov was not confirmed later by Kopylov, therefore we have corrected the results on the Cu_2S-Na_2S-PbS system in accordance with Kopylov's results.

1 Introduction

The copper canister is going to play a very important role for the function of the final repository for high level nuclear waste. From this reason it is also important that statements about its integrity is trueworthy beyond any doubt. Resent reviews of older work and statements about copper has shown that these conditions are not completely fulfilled as the foundation of data is incomplete and in some instances probably also wrong. It has been demonstrated that it is possible to speculate in mechanisms for corrosion attack that are different from those considered earlier. For example it can not be ruled out that sulfide can offer a rapid transport mechanism at corrosion of copper.

From these reasons, properties of copper sulfides and other heavy metal sulfides of relevance for the repository environment are subject for a limited review here.

The work has been carried out as a limited literature review concentrating on the data base INIS. The order of search has been according to the procedure described below and carried as far as the economical frames for the project have permitted. The economical frame have limited both the search efforts and the depth of evaluation and also reporting standards.

Data have been collected concerning:

- General information about sulfides of heavier elements and especially of copper and silver.
- Data about known copper sulfides and about their crystal structure, electrical properties, defects, atom mobility, vacances, stability, phases and crystal formation and growth. (Data about the mobility of copper atoms in sulfide phases are very important).
- Data about copper species formed in water.
- Mechanisms for copper sulfidation in air and water.
- Sulfidation of silver-copper alloys.
- Compilation of thermodynamic data for copper-sulfur species (equilibrium constants and normal potentials)

The search has resulted in much data about copper but less for the other heavy metals. It has not been possible to order reports and articles according to the listing above. The sorting of the material has resulted in the subsequent headings.

2 Sulfide phases and their formation

Under this heading a set of references are accounted where different kinds of information on sulfide phases, and their conditions of formation and existence are accounted. The literature material has a broad spectrum of origin. There are results of studies in gaseous as well as solution environment and also from different areas of purpose as tarnishing in living environment as well as from controlled laboratory environment.

2.1 Tarnishing and atmospheric corrosion

The kinetics of desulfurization of hydrogen sulfide, using metallic copper as desulfurizer, was investigated [1] over a range of temperatures and pressures of hydrogen sulfide. The results indicate that there are two stages of reaction. Activation energies for the first an second stages are 63 kJ/mol and 38 kJ/mol, respectively. Possible reaction mechanisms in which the initial rate is controlled by interface reactions and the later stage is controlled by diffusion through or in the Cu_2S layer are consistent with experimental data.

In [2], the tarnishing of a single phase "14 carat" Au-Ag-Cu alloy was studied. Auger electron spectroscopy and coulometry were employed for the characterization of the composition and the thickness of the surface layers formed. X-ray diffraction was used for further characterization of thicker layers. The layer formation followed linear kinetics. The tarnished layer at short test durations of 0.5 to 5 hours consisted mainly of Ag_2S, CuS and Cu_2S or compounds near to this stoichiometry. The composition of the top surface of the tarnished layer is constant but its global composition changes with the duration of the tarnishing test.

Tarnishing was carried out using an accelerated test (TN test) with immersion of the samples in a solution fixed at 25°C +0.1M Na_2S (pH 14).

The effect of nitrogen dioxide and chlorine on the sulfidation of silver and copper by hydrogen sulfide was investigated in [3] in conditions representative for indoor corrosion, which means low level of gaseous pollutants, no condensation of water vapor and room temperature. Nitrogen dioxide shows oxidative properties against both metals, and may accelerate the process of sulfidation depending on the ratio $p(NO_2)/p(H_2S)$. A similar acceleration of the sulfidation is observed with chlorine on copper and silver. Copper chloride is always obtained, whereas the formation of silver chloride depends on the ratio $p(Cl_2)/(p(H_2S)$. In certain circumstances the formation of silver and copper sulfides has been found to be promoted by the presence of other species as gaseous NO_2 and Cl_2. This situation demonstrates the importance to know the full influence on copper corrosion of all material present in the repository environment.

The tolerance for corrosive damage of metals used in electrical and electronic applications is very low. Atmospheres with high relative humidity and trace levels of pollutant gases can cause tarnishing of metals and adversely affect their electrical properties. In [4] it is demonstrated that already a few monolayers of adsorbed water with some dissolved SO_2 is sufficient to initiate electrochemical corrosion processes on the surface of (silver, copper and gold).

In [5], the tarnishing layers grown on copper exposed to air contaminated by traces of sulfur dioxide and/or hydrogen sulfide were detected by a coulometric and characterized by a chemical method. Depending on the nature of the corrosive gas, or on the use of a gas mixture, it was found that sulfate, sulfide, oxides or a mixed oxide-sulfide compound could be formed under these conditions. The same tarnishing products were found, either in hydrogen sulfide or in a sulfur dioxide - hydrogen sulfide mixture, and the same linear growth law of the copper (I) sulfide was also found. All within the limits of the duration of the corrosion test, in the two gaseous environments as shown in Figure 1.

In [6], the photodoping process in the thin-film light-sensitive structure on the basis of As_2S_3 and Ag layers was investigated. As a result of irradiation, an intermediate doped layer with almost rectangular silver distribution is formed in such a structure. The stimulation of the photodoping process is found to be connected with the irradiation of the borders of such a structure. The excitation of the region near the border, which is doped-undoped As_2S_3 is the most effective. In the light activated silver transfer an important role is played by a photoelectronic process, in particular, by the drift of the photogenerated carriers in the electric fields of interface barriers. The intermediate doped layer is characterized by high silver mobility. At the same time, the parameters of diffusion silver transfer in this layer change only a little under the influence of illumination. The influence of irradiation on silver and copper sulfide nucleation, formation and transportation properties should as a result of these observations be accounted for in the repository environment.

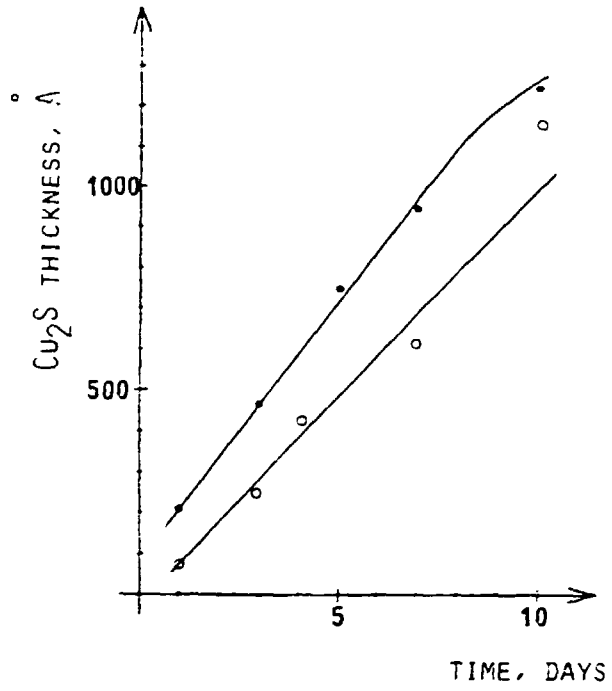

Figure 1
Growth rate of Cu-S on copper samples exposed to corrosive atmospheres: ● - H_2S 0.5 ppmv + 75% R.H.; O - H_2S 0.5 ppv + SO2 1 ppmv + 75% R.H.

Atmospheric corrosion products of copper were identified in [7] by scanning electron microscopy, X-ray microanalysis, X-ray diffraction, and electron diffraction. The samples were exposed to the air for periods of 1/2, 1, 3, and 6 months. The corrosion products were composed of chlorides, sulfur compounds, and oxides. Among them, the constituents identified were Cu_2O, CuCl, $3Cu(OH)_2 \cdot CuCl_2$, and Cu_2S.

The kinetics of copper sulfidation have been studied as a function of temperature (570-1120 K) by the use of the modified Wagner's pellet method [8]. It was found that sulfidation follows a parabolic rate law with different activation energies in the low- and high-temperature ranges. The parabolic rate constants obtained are listed in Tables 1 and 2.

Table 1
Parabolic rate constants for sulfidation of copper and silver at a sulfur pressure of 101.3 kPa, determined by the classical pellet method and with a modified pellet method. $k'_p \times 10^4$ (cm^2s^{-1}).

	Ag_2S, T		Cu_2S, T		
	673 K	723 K	673 K	723 K	823 K
Classical pellet method	2.42 2.45 2.58	2.79 2.82	0.35 0.35 0.34	0.96 0.98	2.54
Modified method	2.41 2.45 2.50	2.85 2.82	0.34 0.36	1.01 0.99	2.52 2.60

Table 2
Parabolic rate constants of copper sulfidation at a sulfur pressure of 101.3 kPa. $k'_p \times 10^4$ (cm^2s^{-1}).

Temperature K	This study	Mrowec	Rickert
573		0.042	
623		0.140	
673	0.35	0.350	0.35
717		0.725	0.66
723	1.00		
773	2.10		
823	2.55		
873	2.80		
923	3.30		
1023	3.60		
1073	3.80		
1123	4.10		

Figure 2 in turn illustrates the temperature dependence of parabolic rate constants of copper sulfidation.

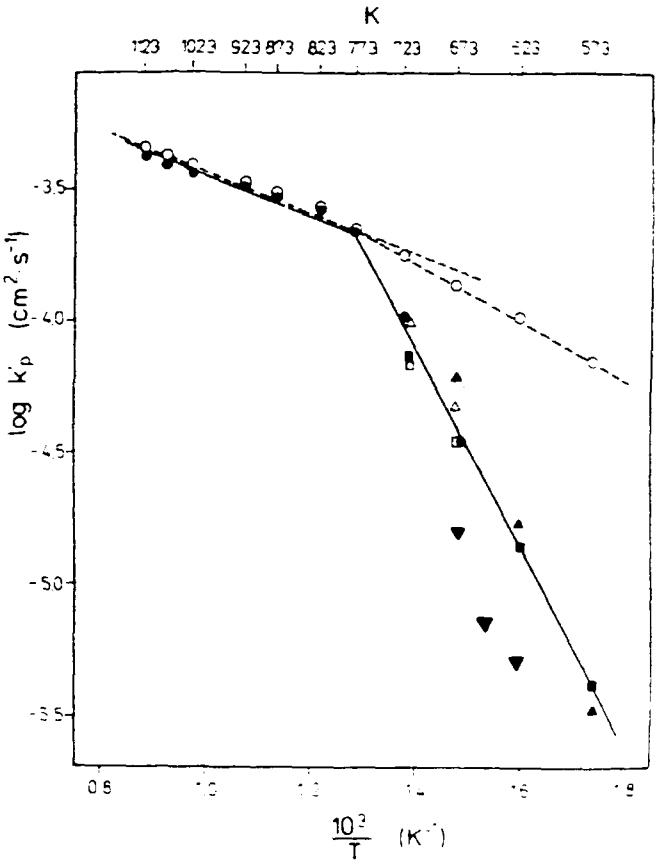

Figure 2
Temperature dependence of parabolic rate constant of copper sulfidation at a sulfur vapor pressure of 101.3 kPa. Results obtained by Mrowec. ☺; this study, ●; this study with a "hexagonal" pellet, ▼; calculated with the assumption of local thermodynamic equilibria at both interfaces, O; calculated with the assumption of an electrical potential at the Cu/Cu_2S interface from the data given by Rickert and Koniew et al, respectively, Δ, ▲.

The obtained values form two straight lines in the Arrhenius plot and can be described as follows:

$k'_p = 10.2\exp\text{-}(70+\text{-}4)[kJ/mole]/RT$ 570-780 K

and

$k'_p = 1.69 \times 10^{-3} \exp\text{-}(13+\text{-}1.0)[kJ/moleJ/\ RT$ 780-1120 K

The change in slope of the curve in the Arrhenius plot (Figure 2) testifies to a complicated mechanism of copper sulfidation. From the copper-sulfur phase diagram, shown in Figure 3, it follows that above 780 K a single-phase sulfide

scale should be formed, consisting of Cu_2S of regular structure, whereas at temperatures from 370 to 780 K it should be a three-phase scale, consisting of hexagonal and regular Cu_2S and CuS.

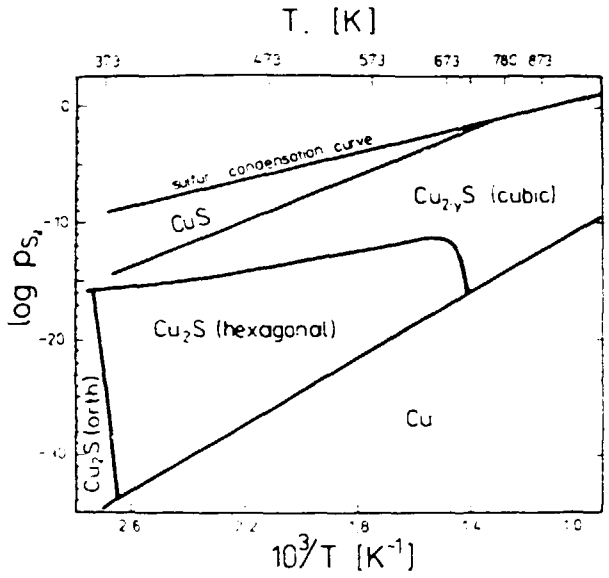

Figure 3
Cu-S phase diagram.

Using thermodynamic data as well as interfacial chemical potentials and ionic conductivity, the parabolic rate constants of sulfidation of copper have been calculated with good agreement with experimental results. Parabolic rate constants of sulfidation have been used to calculate average self-diffusion coefficients of copper in Cu_2S, the temperature dependence of which is shown in Figure 4 and can be written as follows:

$D_{cu} = 8.76 \times 10^{-4}$ exp- (22.4+/-1) [kJ/mole]/RT

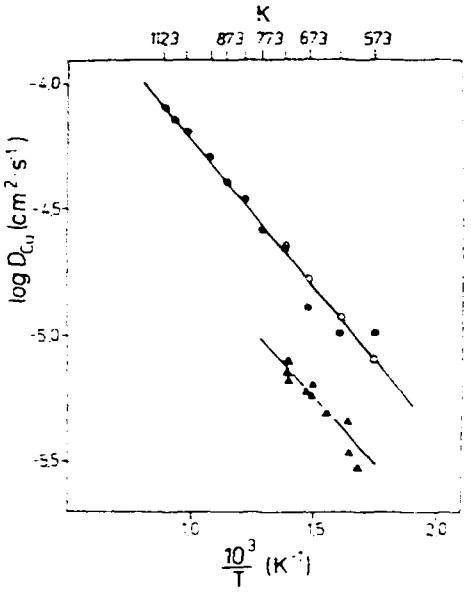

Figure 4
Temperature dependence of self-diffusion coefficient of copper in Cu_2S. Results: ●, calculated from parabolic rate constants of copper sulfidation; O, calculated from ionic conductivity, ▲, radioisotopic studies (Pokrowski et al).

2.2 Processes in solution

The chemical deposition of uniform and adherent Ag_2S films have been studied in [9] from aqueous alkaline baths using thiourea as a sulfur source. The bath temperature was varied from 8 to 55°C and EDTA was used as a complexing agent. Ag_2S films were characterized by XRD, optical absorption and electrical resistivity techniques. The material was later used for the formation of photo-electrical cells. It was demonstrated that the formation of silver (and probably also copper-) sulfide is easy also in the presence of strong complexing agents. In [10] it was demonstrated that in supersaturated solutions, EDTA has been found to inhibit CuS precipitation only for periods of a few hours. The rate of precipitation increases with increasing total copper and sulfide concentrations, but decreases with increasing EDTA/Cu concentration ratio. Colloidal sulfur accelerates precipitation rates in acidic solutions.

The effect of the concentration of dissolved sulfide on the corrosion of Cu-Ni alloys in standard seawater was investigated in [11]. It is seen that the corrosion rates of both Cu-Ni alloys generally increase with increasing sulfide concentrations. As shown in Figures 5 and 6 the result of the present investigation was compared to the data reported in the literature and excellent agreement was obtained in some cases. Possible mechanisms for the acceleration of corrosion was discussed. It was concluded that sulfide acts as a catalyst for both the anodic and cathodic reactions. It is shown that CuS precipitates first and is converted to Cu_2S during the corrosion process.

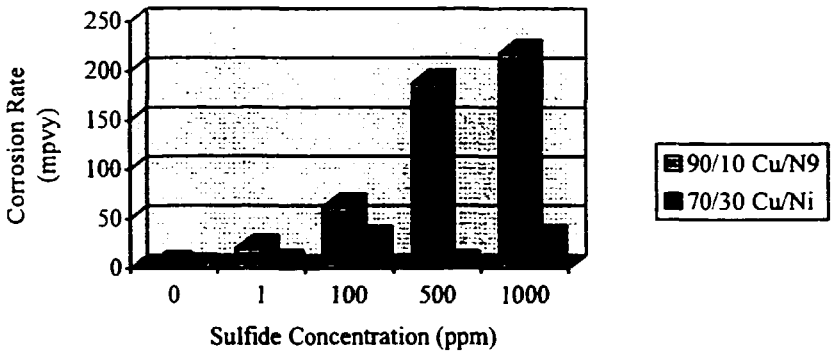

Figure 5
The effect of sulfide concentrations on the corrosion rates of Cu-Ni alloys in seawater under aerated and stirred conditions.

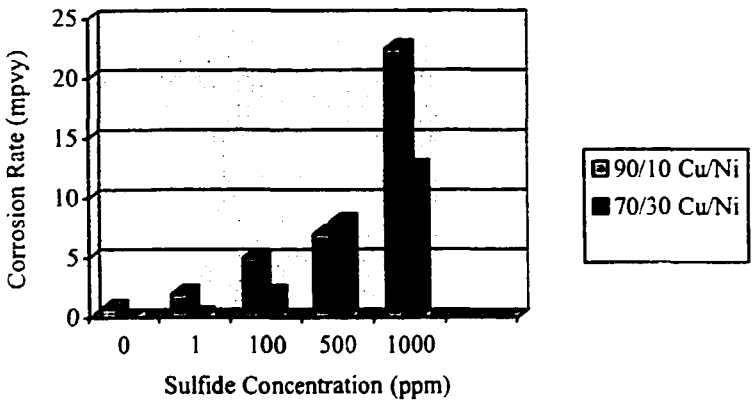

Figure 6
The effect of sulfide concentrations on the corrosion rates of Cu-Ni alloys in seawater under aerated and stagnant conditions.

In [12] it is demonstrated that the precipitation of crystalline CuS (covellite) is kinetically inhibited in the presence of amonocarboxylate chelating agents, EDTA and DCTA, even in highly supersaturated solutions. At millimolar concentrations at pH 8.1, these chelating agents adsorb strongly enough to CuS

surfaces to approach monolayer coverage, reaching a density of about one molecule per 80 $Å^2$. Bisulfide competes with the chelators for surface sites. Growth of CuS was studied turbidimetrically by mixing solutions of chelated copper with bisulfide solutions in a stopped-flow spectrophotometer. The data were well fit by a rate law:

$$d[CuS]/dt = kA\theta_{HS}[CuY]$$

where k = rate constant, A = particle surface area per unit volume of solution, θ_{HS} = fractional coverage of surface sites by sulfide, rather than chelator, and [Cu Y] = concentration of copper chelate in solution. This rate law suggests that growth is controlled by encounters between HS, bound to the surface and chelated copper from the solution. Growth is diffusion limited. Differences in k obtained when Y = EDTA and DCTA suggest that only forms of the chelated copper with coordination number less than 6 are kinetically active.

In [13], the phase equilibria of the copper-sulfur system were investigated using electrochemical cells from 0° to 250°C over the composition range Cu/S = 0.95-2.10. Vapor-saturated aqueous cupric sulfate and cuprous chloride solutions were used as the electrolytes. The two blaubleibender covellites, low digenite, a nameless tetragonal phase and protodjurleite were found to be metastable. The $Cu_{1.9}S$ phase was demonstrated not to be a real phase in the system. The stable invariant points were as shown in Table 3.

Table 3
Summary of stable invariant points. Compositions are in Cu/S ratio.

T °C	Covellite	Anilite	High digenite	Djurleite	Low chalcocite	High chalcocite	Additional phase
507±2	1.000±0.001	-	1.732±0.005	-	-	-	+ sulfur
435±8	-	-	2.000±0.0038	-	-	2.000±0.0038	+ copper
103.5±0.5	-	-	-	-	2.000±0.002	2.000±0.002	+ copper
93±2	-	-	1.834±0.002	1.942±0.002	-	1.988±0.005	-
90±2	-	-	-	1.960±0.002	1.993±0.002	1.990±0.005	-
75±3	1.000±0.001	1.750±0.003	1.765±0.002	-	-	-	-
72±3	-	1.750±0.003	1.805±0.002	1.934±0.002	-	-	-

2.3 Structures and phase relations

In [14] additional x-ray structure studies on low chalcocite generally confirm the previously reported structure but show that either disorder is present or the true space group is not $P2_1/c$ but Pc.

It is demonstrated in [15] that low chalcocite has a monoclinic space group $P2_1/c$, with a unit cell having a= 15.246(4)Å, b= 11.884(2)Å, c= 13.494(3)Å, β= 116.35(1)°, and containing 48 Cu_2S. The structure is based on a hexa-

gonal-close-packed framework of sulfur atoms, with copper atoms occupying mainly triangular interstices. Of the 24 different copper atoms, 21 form triangular CuS_3 groups, and one is in a distorted CuS_4 tetrahedron.
Djurleite is monoclinic, space group P21/n, with a unit cell having a = 26.897(6)Å, b = 15.745(3)Å, c = 13.565(3)Å, β = 90.13(3)°, and containing 8 $Cu_{31}S_{16}$. The structure is similar in general to the low chalcocite structure, but of the 62 different copper atoms, 52 form triangular groups, 9 form distorted tetrahedral groups, and one is in unique linear twofold coordination.
Both structures are derived from the high chalcocite structure (P 6_3/m, a = 3.96Å, c = 6.72Å, cell content = $2Cu_2S$) which forms a substructure corresponding to the hexagonal-close-packed sulfur framework. The details of the copper arrangement are entirely different in the two phases. The average Cu-S bond length in the CuS_3 triangles is 2.32Å in low chalcocite and 2.29 Å in djurleite. The overall average Cu--S distance in the tetrahedral is 2.48 Å, but varies from 2.22 to 2.91 Å. Each copper atom has from 2 to 8 other copper atom neighbors less than 3.0 Å distant, varying up from 2.45 Å, through a maximum clustering at about 2.78 Å. Cu-Cu bonding interaction is probably significant but is not clearly understood.

The phase state of the Cu_2S--FeO system was investigated in [16] at temperatures up to 1450 °C and gas phase oxygen partial pressures in the range 10^{-1} - 10^{-7} Pa. The constructed phase diagram is shown in Figure 7.

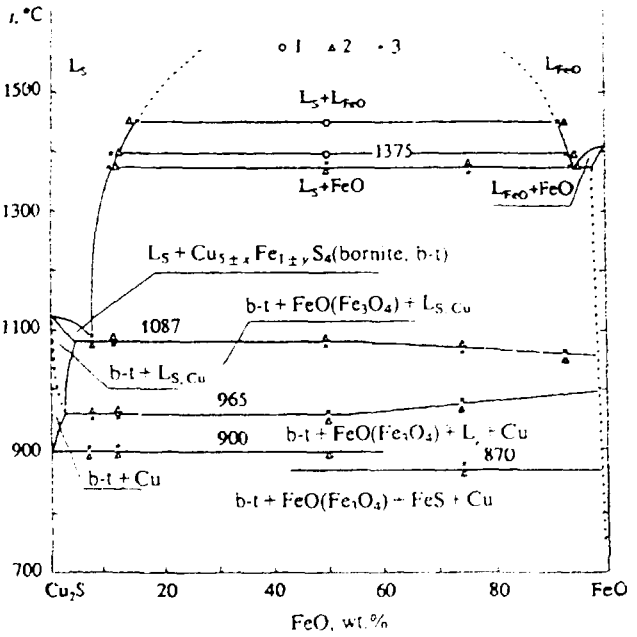

Figure 7
Phase diagram for the Cu_2S-FeO system: 1, data points for the original study; 2, experimental data at oxygen partial pressures over the melt in the range 10^{-1} - 10^{-2} Pa; 3, ditto in the range 10^{-4} - 10^{-7} Pa.

2.4 Microbially induced corrosion

In [17] mineralogical data, thermodynamic stability (Pourbaix) diagrams, and the simplicity principle for precipitation reactions were used to evaluate corrosion product mineralogy on copper alloys exposed to sulfate-reducing bacteria. The formation of copper sulfides as corrosion products in natural surface environments is suggestive of microbiologically influenced corrosion. Sulfide corrosion products other than chalcocite (Cu_2S) indicate that reactions within a biofilm induced corrosion. Figure 8 shows a copper-sulfur stability diagram for 10^{-2} M total sulfide concentration incorporating thermodynamic data for chalcocite (Cu_2S) and covellite (CuS).

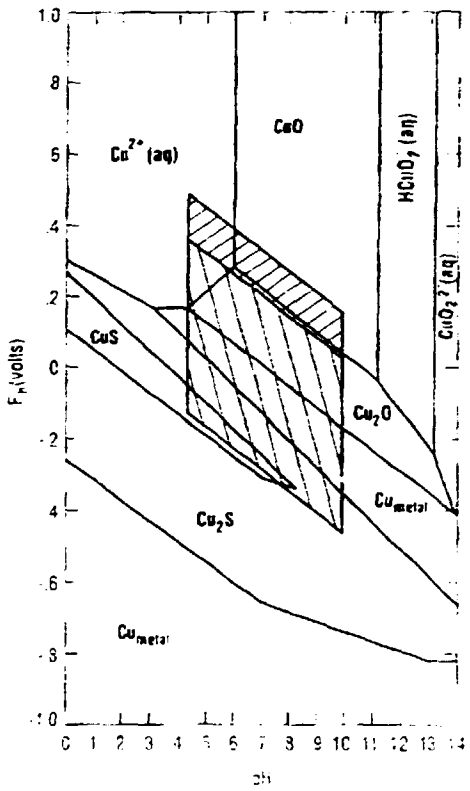

Figure 8
Thermodynamic stability diagram for copper in fresh water with parallelograms bounding natural environmental conditions. Total reduced sulfide = 10^{-2} M; total dissolved copper = 10^{-6} M.

2.5 Some important observations

- At desulfurization of hydrogen sulfide with metallic copper two stages of reaction are observed with activation energies for the first an second stages are 63 kJ/mol and 38 kJ/mol, respectively. Suggested mechanisms are initial interface reactions and a later stage which is controlled by diffusion through or in the Cu_2S.

- At tarnishing of an Au-Ag-Cu alloy the layer formation followed linear kinetics. Ag_2S, CuS and Cu_2S are formed.

- The formation of silver and copper sulfides is promoted by NO_2 and Cl_2. NO_2 can be formed at radiolysis in the canister environment.

- A few monolayers of adsorbed water with some dissolved gases are sufficient to initiate electrochemical corrosion processes on silver and copper.

- Atmospheric corrosion products of copper were identified as Cu_2O, CuCl, $3Cu(OH)_2 \cdot CuCl_2$, and Cu_2S.

- The existence of light-sensitive structures based on Ag and Cu sulfides show the importance of irradiation in sulfide related processes.

- In high temperature ranges (>300 °C) the kinetics of copper sulfidation follow a parabolic rate law. Rate constants have been used to calculate average self-diffusion coefficients of copper in Cu_2S.

- The formation of silver (and probably also copper-) sulfide is easy also in the presence of strong complexing agents.

- Sulfide acts as a catalyst for both the anodic and cathodic reactions on copper. It is shown that CuS precipitates first and is converted to Cu_2S during the corrosion process.

- Bisulfide has a high affinity for copper and competes with the chelators for surface sites on CuS

- Low chalcocite (Cu_2S) is monoclinic and the structure is based on a hexagonal-close-packed framework of sulfur atoms, with copper atoms occupying mainly triangular interstices. Djurleite is monoclinic and the structure is similar in general to the low chalcocite structure. Both structures are derived from the high chalcocite structure which forms a substructure corresponding to the hexagonal-close-packed sulfur framework. The details of the copper arrangement are entirely different in the two phases.

- The formation of copper sulfides as corrosion products in natural surface environments is suggestive of microbiologically influenced corrosion.

3 Diffusion and diffusion routes

3.1 General

The structure of the antifluorite-type copper chalkogenides Cu_2Se and $Cu_{1.8}S$ were studied in [18] by using single crystal X-ray diffraction data both below and above the transition point. The average structures of the compounds were refined and a face centered arrangement of the chalcogen atoms was assumed. Copper atoms were distributed at the tetrahedral, trigonal, and octahedral interstitial sites, and their relative populations were refined. The tetrahedral and trigonal sites are populated by copper atoms in both room temperature and high temperature phases. The octahedral site is not populated in the room temperature phase of either Cu_2Se and $Cu_{1.8}S$. Contrary to EXAFS analysis results, however, this site is populated in the high temperature phase of Cu_2Se. From the population data, the drift pathway of copper ions was discussed.

In [19] Cu_2S-CdS heterojunctions were studied by using SIMS and other methods. Diffused Cu reached about 25 μm in depth from the junction interface and the Cu diffused area was observed directly by using SIMS and other methods for depth profiling. The temperature dependence of the diffusion coefficient was determined.

The following relation was obtained.

$$d^2/t=0.46 \times \exp(-0.96)\ eV/kT)\ cm^2/sec$$

The activation energy is 0.96 eV.

A phase diagram of the system Cu_2S-FeS-FeO is plotted [20].

The use of point electrodes for measuring chemical diffusion coefficients of mixed conducting solids with prevailing electronic conductivity is described and applied to low temperature Cu_2S in [21]. The measurements on the low temperature phase of Cu_2S give chemical diffusion coefficients ranging between $6*10^{-6}$ cm^2 /s and $1*10^{-7}$ cm^2/s at 60°C. The temperature dependence for three different samples is given in Figure 9.

A survey, comparison, and critical analysis is presented in [22] of data compiled from the scientific literature concerning diffusion in copper-silver and copper-gold systems. The term "copper alloy system" is interpreted in the broadest sense. For example, the review of diffusion in the Cu-M system reports all diffusion situations which involve both copper and element M, including diffusion of Cu in M or in any binary, ternary, or multicomponent alloy containing M: diffusion of M in Cu or in any alloy containing Cu; and diffusion of any element in any alloy containing both Cu and M. Topics include volume diffusion, surface diffusion, grain boundary diffusion, tracer diffusion, alloy interdiffusion, electromigration, thermomigration, strain enhanced diffu-

sion, and diffusion in molten metals. An extensive bibliography is presented along with figures, tabular presentation of data and discussion of results.

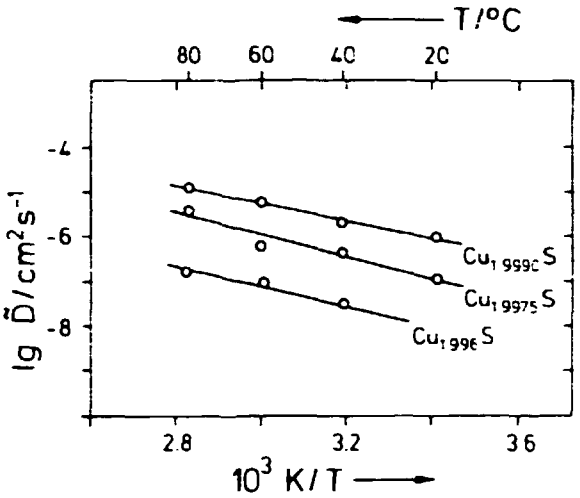

Figure 9
Temperature dependence of the chemical diffusion coefficient of the three sample compositions $Cu_{1.999}S$, $Cu_{1.9975}S$, $Cu_{1.996}S$.

The diffusion coefficient of silver in pure copper is shown in Figure 10 as a function of temperature.

The different coefficients of gold in pure copper is shown in Figure 11 as a function of temperature.

In [23], chemical diffusion coefficients of mixed conducting low temperature phases of copper selenide and copper sulfide between 20°C and 80°C are accounted, measured by a method which makes use of inert point electrodes. Earlier results on chalcocite (Cu_2S) were reproduced and extended. The electrochemical cell consisted of the phase sequence $Pt/Cu_xY(Y=S,Se)/Pt$-point electrode. Chemical diffusion coefficients were evaluated from the time dependence of the ohmic resistance after an instant change of voltage or current. For example at 20°C, chemical diffusion coefficients were obtained which for chalcocite (Cu_2S) range between $1*10^{-6}$ and $1.3*10^{-8}$ cm^2/s, and for β-Cu_2Se between $2.4*10^{-6}$ and $4.3*10^{-7}$ cm^2/s, whereas djurleite ($Cu_{1.95}S$) shows only slightly varying values between $1.4*10^{-8}$ and $2.4*10^{-8}$ cm^2/s.

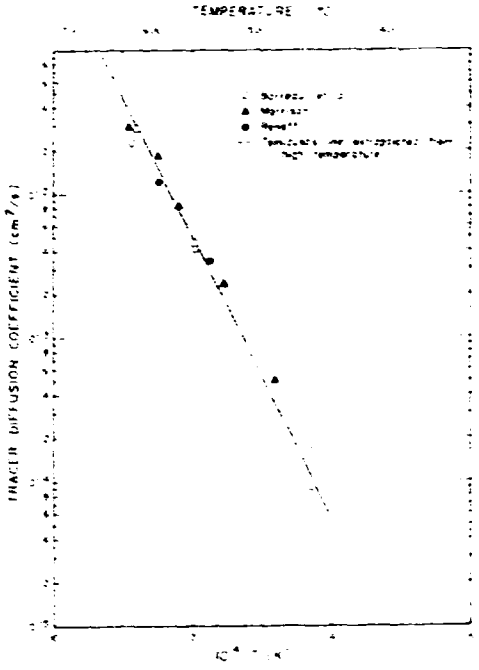

Figure 10
Tracer diffusion coefficients of silver in pure copper as a function of the reciprocal absolute temperature.

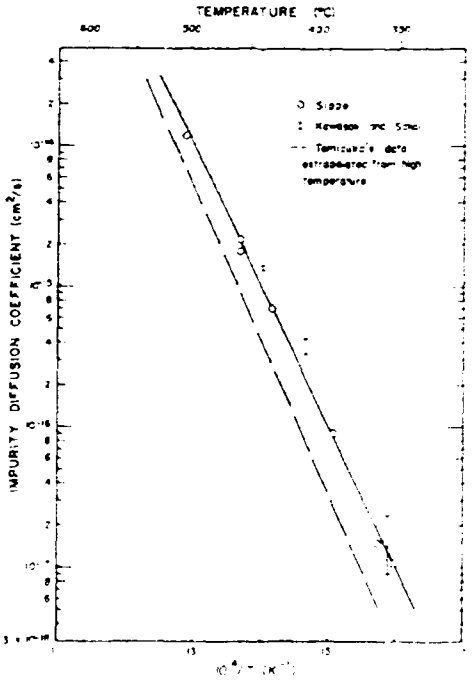

Figure 11
Impurity and tracer diffusion coefficients of gold in pure copper (at low temperatures, 500 to 350°C) as a function of reciprocal absolute temperature.

The chemical diffusion coefficient in the low temperature chalcocite phase is shown in Figure 12. A very strong dependence on composition is seen.

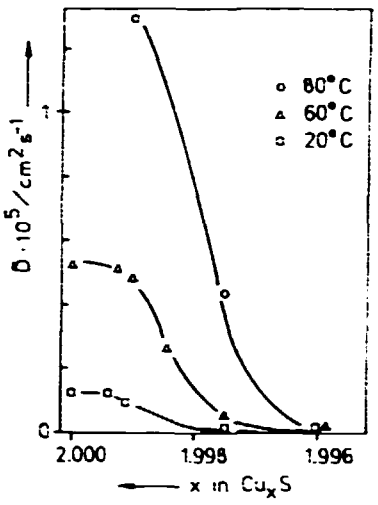

Figure 12
Chemical diffusion coefficient of low temperature Cu_xS as a function of composition: $2.000 > x > 1.995$.

The temperature dependence of the chemical diffusion coefficient is shown in Figure 13. These lines gives an activation energy parameter of 0.32±0.02 eV for djurleite and 0.45±0.05 eV for chalcocite.

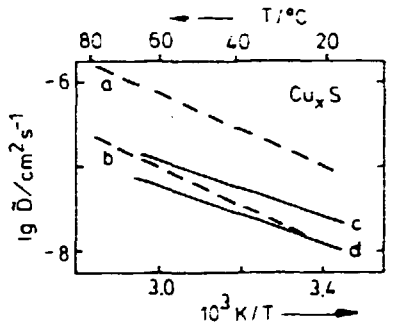

Figure 13
Temperature dependence of the chemical diffusion coefficient of low temperature Cu_xS.
-- chalcocite: a-$Cu_{1.9975}S$, b-$Cu_{1.996}S$
__ djurleite: c-$Cu_{1.957}S$, d-$Cu_{1.930}S$

In [24], the zonation, exsolution and replacement phenomena occurring in natural sphalentes and known as the "chalcopyrite disease" were experimentally

simulated by solid-state diffusion studies using (Zn,Fe)S crystals as receptors and $CuInS_2$, $CuFeS_2$, Cu_5FeS_4, $Cu_{2-x}S$ and CuS as metal sources, at temperatures between 400 and 750°C. Therefore, the expression "diffusion-induced segregations" (DIS) is proposed instead of "disease". The driving force for the diffusion is a chemical-potential gradient between the sphalente crystal (receptor) and the surrounding sulfide powders (diffusion source). Diffusion coefficients of (Cu+In) in ZnS were experimentally determined. The nature of the DIS phases (intermediate solid solution, chalcopyrite, bornite, digenite) and the corresponding textures (dusty, blebs, worm-like, water-melon) depend on the Fe content of the sphalente, time, temperature, Cu:Fe ratio in the diffusion source, and the sulfur fugacity. General rules for DIS phenomena are deduced from the experimental results and compared to natural occurrences. All the natural "disease" textures of Cu-rich phases in sphalerite was reproduced.

The structures of the antifluorite-type copper chalcogenides Cu_2Se and $Cu_{1.8}S$ were studied in [25] using single crystal X-ray diffraction data both below and above the transition point. Using the cubic indexing main reflections, the average structures of the compounds were refined by least squares methods. A face centered arrangement of the chalcogen atoms was assumed and copper atoms were distributed at the tetrahedral, trigonal, and octahedral interstitial sites and their relative populations were refined. The tetrahedral and trigonal sites are populated by copper atoms at both room temperature and high temperature phases. The octahedral site is not populated in the room temperature phase of either Cu_2Se and $Cu_{1.8}S$. Contrary to the EXAFS analysis, however, this site is populated in the high temperature phase of Cu_2Se. From the population data, the drift pathway of copper ions was discussed.

The activation energy for copper diffusion is reported as being about 0.24 eV for both Cu_2Se and Cu_2S.

A model for the mobile copper ion disorder in hexagonal Cu_2S between 120° and 325°C has been established [26] by single crystal neutron diffraction. The copper ions partially occupy two sets of three-coordinated sites within the HCP sulfur array and display anharmonic thermal motion. The results suggest that the conductivity is two dimensional in nature.

In [27], the structures of the fast ion conductors Cu_2Se, $Cu_{1.8}Se$ and $Cu_{1.8}S$ was studied with the use of single crystal X-ray diffraction data. The compounds have cubic antifluorite structures. The copper ions are distributed to the tetrahedral, trigonal and octahedral interstitials of the chalcogen atoms. In the refinement of the structures, the maximum entropy method (MEM) is used to construct the density map of the copper ions. The distribution of the copper ions is studied as a function of temperature. The diffusion path of the mobile copper ions is also discussed.

The effect of copper diffusion from the p-Cu_2S into the n-CdS region, due to heat treatment, in a Cu_2S/CdS heterojunction photovoltaic cell is discussed in [28] from a theoretical standpoint. The technique employs the energy band dia-

gram resulting from a modified Schottky barrier in the CdS and the solution of the one-dimensional Poisson's equation with appropriately assumed boundary conditions and a diffusion model of Gaussian profile for the Cu-acceptor concentration in the CdS.

Quantitative growth of thin Cu_2S layers in chemiplated thin film CdS:Cu_2S solar cells was observed [29] by studying the depth profile concentrations of copper and sulfur by the X-ray photoelectron spectroscopy technique. Scanning electron microscopy examination of the junction revealed a complex and corrugated structure at the interface. From a study of the spatial distributions of cadmium, copper and sulfur and measurements of the saturated [Cd]/[S] ratios, it is inferred that in deep layers the copper originates from grain boundaries. Similarly, by isolating the copper profile in the Cu_2S layers, the CdS grain-grain boundary region and the CdS grain boundaries and by applying suitable diffusion equations with appropriate boundary conditions, the diffusion coefficients in the midgrain and grain boundary regions were evaluated. In the chemiplating process copper diffusion is $5 \cdot 10^2$ times faster in the grain boundary than in midgrain. A short heat treatment of the cells causes the redistribution of cadmium and copper in the junction, making the interface sharper. Analysis yields diffusion coefficients of $5.8 \cdot 10^{-11} \exp(-0.229/kT)$ in midgrain and $1.06 \exp(-0.964/kT)$ in the grain boundary. In order to gain knowledge of the degradation effects arising from copper migration, the evaluated diffusion coefficients were used to compute the time in which loss of Cu_2S stoichiometry and widening of the copper-compensated layer will lead to significant reduction in cell performance.

3.2 Some important observations

- In Cu_2Se and $Cu_{1.8}S$, copper atoms are distributed at the tetrahedral, trigonal, and octahedral interstitial sites both at room temperature and high temperature. The octahedral site is not populated at room temperature. From the population data, the drift pathway of copper ions are discussed.

- Temperature dependence of the diffusion coefficient is determined and a mathematical relation is given. The measurements on the low temperature phase of Cu_2S give chemical diffusion coefficients ranging between $6*10^{-6}$ cm^2/s and $1*10^{-7}$ cm^2/s at 60°C.

- A survey is made of diffusion data in copper-silver and copper-gold systems. Topics include volume diffusion, surface diffusion, grain boundary diffusion, tracer diffusion, alloy interdiffusion, electromigration, thermomigration, strain enhanced diffusion, and diffusion in molten metals. An extensive bibliography is presented along with figures, tabular presentation of data and discussion of results.

- Chemical diffusion coefficients at 20 °C were obtained which range for chalcocite (Cu_2S) between $1*10^{-6}$ and $1.3*10^{-8}$ cm^2/s, and for β-Cu_2Se

between $2.4*10^{-6}$ and $4.3*10^{-7}$ cm^2/s, whereas djurleite ($Cu_{1.95}S$) shows only slightly varying values between $1.4*10^{-8}$ and $2.4*10^{-8}$ cm^2/s.

- At growth of thin Cu_2S layers in chemiplated thin film CdS, the diffusion coefficients are $5*10^2$ times larger in the grain boundary than in midgrain.

4 Solubility

4.1 General

The solubility of Au_2S at 25°C in aqueous H_2S-HS^- solutions were measured in [30] from pH 2 to 12 and over a range of reduced sulfur concentrations from 0.005 to 0.4 molal. The species $AuHS^0$, $Au(HS)_2^-$ and $Au_2S_2^{2-}$ were identified and thermodynamic solubility constants were derived for the reaction

$$Au_2S+(2(n+z)/x-1)HS^- = 2/xAu_x(HS)_nS_z^{(x-n-2z)} + (2z/x-1)H^+$$

using a nonlinear least squares procedure with the following results: log $K_{Au,110}$ = -6.68 (0.03) for $AuHS^0$; log $K_{Au,120}$ = +4.52 (0.01) for $Au(HS)_2^-$; and log $K_{Au,202}$ = -14.63 (0.03) for $Au_2S_2^{2-}$. The quoted uncertainty corresponds to one standard deviation. The first dissociation constant for H_2S obtained from the Au_2S solubility measurements was log K_{a1} = -6.98 (0.01). From published high temperature and pressure values of K_{r120} for the reaction

$$Au_{(c)} + H_2S + HS^- = Au(HS)_2^- + H_{2(g)}$$

the following standard partial molar volume of $Au(HS)_2^-$ was obtained: 175 °C, -36; 200 °C, -25;225 °C, -10; and 250 °C, -15. Published solubility data for Ag_2S in solutions at I =1.0 and 20°C have been reinterpreted to give the following thermodynamic solubility constants at infinite dilution: log $K_{Ag,110}$ = -8.94 (0.01) for $AgHS^0$; log $K_{Ag,120}$ = -1.02 (0.01) for $Ag(HS)_2^-$; and log $K_{Ag,221}$ = -4.44 (0.01) for $Ag_2(HS)_2S^{2-}$.

The solubility of covellite has been measured in 0.5-2.0 M NaCl at 25°C. Solutions containing various concentrations of total sulfide and zerovalent sulfur were studied over the pH range 6-11. The data are interpreted in the terms of the following complexes, for which stability constants are presented: $CuS(HS)_2^{2-}$, $CuS(HS)_3^{3-}$, $Cu(S_5)_2^{3-}$, $Cu(S_4)(S_5)^{3-}$, and $CuS(S_5)^{2-}$.Three out of these five species have not been reported before and are probably of importance in anoxic natural waters. The three complexes with the general formula, $CuS(X)_n$ do not display optical absorption spectra characteristics of Cu(II) even though the oxidation state of copper, by convention, is divalent. When Cu^{2+} and S^{2-} combine to form the CuS moiety in these complexes, internal electron transfer from S to Cu occurs. Because polysulfide complexes are extremely stable, the solubility of copper in sulfidic waters is strongly dependent on the activity of solid sulfur, a_S^0. For natural waters, a_S^0 can be calculated from measurements of pH, total zerovalent and total divalent sulfur. At a_S^0 >0.1, polysulfide complexes (especially $CuS(S_5)^{2-}$) are probably the predominant copper species in most sulfide marine waters. Calculated total copper concentrations in equilibrium with covellite agree satisfactorily with published measurements for some Delaware salt marsh pore waters. This agreement is achieved by postulating that Cu-Fe-S phases, such as chalcopyrite, fail to nucleate at low temperatures in nature.

The solubility of Ag_2S (acanthite/argentite) was measured in [31] in vapor saturated aqueous sulfide solutions at 25-300 °C, total sulfide = 0.2 - 1.4 μ, and $pH_{25°}$ = 5.8 - 7.3. Under these conditions, Ag_2S was found to dissolve according to the following reaction:

$$1/2\ Ag_2S(s) + 1/2\ H_2S(aq) + HS^- = Ag(HS)_2^-$$

For which the following logK's were obtained: -3.82+/-0.10(25 °C), -3.26+/-0.10(100 °C), -2.91+/-0.10(150 °C), -2.55+/-0.10(200 °C), -2.32+/-0.10(250 °C), and -2.11+/-0.10(300 °C). These data are in good agreement with previous work at 20 °C (Schwarzenbach and Widmer, 1966) and 100-180 °C (Melent'yev et al, 1969), but not with the dinuclear complex stoichiometries recently obtained by Sugaki et al (1987).

Although Seward (1976) has shown that considerable silver can be dissolved as chloride complexes, the present data indicate that $Ag(HS)_2^-$ is the dominant silver species in hydrothermal fluids with near neutral to alkaline pH, relatively low oxidation state, high total sulfide, and T < 300 °C (e g. Broadlands, N Z; Brown, 1986). Silver transported as $Ag(HS)_2^-$ is precipitated in response to a decrease in aqueous sulfide concentration, a change in pH away from the pK_1 for H_2S, or, in the native silver field, a decrease in the oxidation state. Cooling is a less important depositional mechanism, particularly for solutions whose pH is buffered by the feldspar alteration reactions.

In [32], the equilibrium constant at 25 °C for the following reaction has been measured in NaCl media by an indirect method:

$$CuS(cov) + H^+(aq) = Cu^{2+}(aq) + HS^-(aq), \quad K_{sp} = M_{Cu2+}M_{HS-}(10^{+pH})$$

Where CuS(cov) designates synthetic covellite. Values of pK_{sp} are 21.39, 21.04, and 20.95 at NaCl = 0.2, 0.7, and 1.0 M, respectively. The uncertainty in these K_{sp} values is +/- 0.15. The free energy of formation of covellite, fc. which published values are discordant, is calculated to be -11.83+/- 0.4 kcal/mole at 298 K (-49.50 +/- 1.7 kJ/mole). This value is obtained by extrapolating the measured pK_{sp} values to infinite dilution with correction for Cl^- complexing. Applying similar Cl^- complexing corrections, based on recent measurements by Seward, to previously published solubility data for galena, yields a revised pK_{sp}^0 for galena of 12.78. A poorly crystalline precipitate, obtained by mixing Cu^{2+} and HS^- solutions, yielded a reversible solubility product 3 orders of magnitude greater than that of covellite, but about 3 orders of magnitude less than that of a truly amorphous phase, super cooled liquid CuS. The poorly crystalline phase has not been studied previously. Its bulk composition was $Cu_{1.18}S$, but microprobe analysis revealed that it was a partially exsolved mixture of roughly $Cu_{1.11}S$ and $Cu_{1.32}S$ (similar to known blaubleibender covellites). It was kinetically unstable, and converted to covellite when thermally annealed or when exposed to polysulfide solutions. Because of its instability, a material of this nature is unlikely to account for the amorphous copper sulfide alleged to occur in the Red Sea brine deposits. However, it is

possible that on short time scales dissolved Cu in sulfidic waters is controlled by metastable, rather than stable phases, as is known to be the case with dissolved Fe.

The mechanism of the reactions taking place in the heterogeneous system: synthetic polydispersive Cu_2S--ethylenediaminetetraacetic acid (EDTA)-O_2-H_2O has been investigated [33]. The partial pressure of oxygen and pH of the solution were found to exert a significant effect on the process kinetics. The dissolution rate does not depend, in practice, on the agitation rate and the EDTA concentration exerts an influence only at higher partial oxygen pressures. Dissolution of Cu_2S in aqueous EDTA solutions proceeds in two steps with the formation of CuS as an intermediate. In acid and neutral solutions the final products of dissolution are elementary sulfur and $Cu(EDTA)^{2-}$ complex ion. The activation energy ΔE = 10.4 kJ/mol (2.4 kcal/mol) suggests a diffusion controlled process. In alkaline solutions sulfur is oxidized to the sulfate ion and the dissolution process is kinetically controlled, ΔE= 41.4 kJ/mol (9.9 kcal/mol).

The two step dissolution curves are shown in Figure 14. Further dissolution proceeds at a lower rate and after 50% Cu_2S has been dissolved, the process rate is much lower because of the formation of CuS that does not dissolve so well.

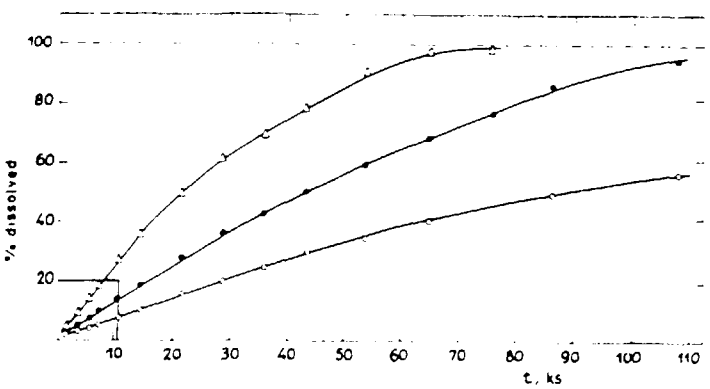

Figure 14
Dissolution curves of Cu_2S. Solution conditions: T = 2930.1 K, c_{EDTA} = 0.19 M, stirring speed = 10 r/s. o, pH = 4.6 and p_{O2} = 0.021 MPa; •, pH = 11.8 and p_{O2} = 0.021 MPa; Δ, pH = 11.8 and p_{O2} = 0.10±0.01 MPa.

The kinetics of copper leaching from a chalcocite-covellite ore have been investigated [34]. Leaching was carried out in sulfuric acid solution at different pH values and particle sizes, in the presence of ferric sulfate leached from the ore. Three stages of leaching were established. The apparent activation energy shows a dependence on the period of leaching and the pH value of the solution. An attempt was made to determine the rate-determining steps according to both the activation energies and the analytical expressions for each period.

A rotating disc electrode (RDE) system was designed for the study of electrochemical leaching kinetics of copper sulfide in acidified ferrous/ferric solutions [35]. A technique was developed for producing hard, machinable and polishable cuprous sulfide disc electrodes of extremely low porosity and incorporating these in circuitry of acceptably low resistance. Sample anodic and cathodic polarization curves are shown and discussed.

4.2 Some important observations

- Published solubility data for Ag_2S in solutions at I =1.0 and 20 °C have been reinterpreted to give the following thermodynamic solubility constants at infinite dilution: log $K_{Ag.110}$ = -8.94 (0.01) for AgHS; log $K_{Ag.120}$ = -1.02 (0.01) for $Ag(HS)_2^-$; and log $K_{Ag.221}$ = -4.44 (0.01) for $Ag_2(HS)_2S^{2-}$.

- The solubility of Covellite has been measured in 0.5-2.0 M NaCl at 25 °C. The data are interpreted in terms of the following complexes, some of which contain polysulfides and for which stability constants are presented: $CuS(HS)_2^{2-}$, $CuS(HS)_3^{3-}$, $Cu(S_5)_2^{3-}$, $Cu(S_4)(S_5)^{3-}$, and $CuS(S_5)^{2-}$.

- Polysulfide complexes are extremely stable. At a_S^0 >0.1, polysulfide complexes (especially $CuS(S_5)^{2-}$) are probably the predominant copper species in most sulfide marine waters.

- The solubility of Ag_2S (acanthite/argentite) was determined and for 25-300 °C, total sulfide = 0.2 - 1.4 μ, and pH_{25} = 5.8 - 7.3, logK´s were obtained to be 3.82+/-0.10(25 °C), -3.26+/-0.10(100 °C), -2.91+/-0.10(150 °C), -2.55+/-0.10(200 °C), -2.32+/-0.10(250 °C), and -2.11+/-0.10(300 °C).

- Values of pK_{sp} for covellite, CuS, are 21.39, 21.04, and 20.95 at NaCl = 0.2, 0.7, and 1.0 M, respectively. The uncertainty in these K_{sp} values is +/- 0.15. The free energy of formation of covellite, for which published values are discordant, is calculated to be -11.83+/- 0.4 kcal/mole at 298 K (-49.50 +/- 1.7 kJ/mole).

5 Thermodynamics

5.1 Data

Nonlinear electrochemical phenomena were observed [36] during reduction of H_2O_2 at $CuFeS_2$ cathodes. The dynamic current-voltage curve from -1.0 to 0.0 Vsce appears N-shaped with a pronounced current wave. If the potential is set constant in the region of the wave, sudden current spikes are observed. A remarkable feature is the onset of sustained current oscillations in the presence of a suitable resistance in series to the working electrode. Frequency and amplitude of oscillations are influenced by the resistance value and by mass transport. A potential modulation of small amplitude may trigger oscillations of the same frequency. Investigations performed with electrochemical techniques show that the phenomena are associated with corrosion of the electrode surface. It is proposed that the observed increases of the current originate from activation of a catalytic mechanism of H_2O_2 reduction involving copper species. A qualitative model is proposed on the basis of circuit analysis which accounts for the main aspects of the oscillating phenomena, including the role of the resistance and the effect of potential stimuli. The requirements for a more thorough kinetic treatment are discussed.

By means of the emf measurement method with solid state galvanic cells, $\Delta fG^\circ m$, $\Delta fH^\circ m$ and $\Delta fS^\circ m$ of Ag_2S and CuS phases were determined in [37]. Some apparent discrepancy on $\Delta fG^\circ(CuS)$ was found which is explained on the basis of the presence of a narrow solubility range of a third component according to previous results obtained with the [(1-x-y)Ag+xCu+yS] system.

Thermodynamic information for copper compounds and aqueous species, including estimated values at elevated temperatures, is analyzed in [38]. Potential pH-diagrams (Pourbaix diagrams) for the Cu - H_2O, Fe - H_2O and Fe - Cu - H_2O systems are presented and the solubilities of copper and iron oxides (including mixed copper-iron oxide) are evaluated. These results are used to interpret the observed precipitation of oxides on BWR fuel and to estimate the effect of hydrogen water chemistry on their behavior.

In [39], thermochemical data are used to construct a modified log-activity diagram for the system Cu-H-O-Cl-(CO_2). This diagram, restricted to standard state of pressure and temperature, serves as a complement to Pourbaix diagrams for the study of equilibria appropriate to solid phases and aqueous ionic species of copper in chloride-bearing waters. Coordinate axes represent activities of chloride and aqueous copper species. Other thermodynamic variables are collapsed onto the diagram. Equilibria involving chlorination reactions, some of which cannot be displayed on a Pourbaix diagram, are presented. Also displayed are the various permissible geometric relationships of lines on a Pourbaix diagram. Modified log-activity diagrams may be used to model localized corrosion of copper and are potentially useful for the analysis and prediction of failure mechanisms in high level waste packages.

In [40], the heat capacities of $Cu_{1.90}S$, $Cu_{1.95}S$, $Cu_{1.98}S$ and $Cu_{1.995}S$ have been measured by adiabatic-shield calorimetry. All samples have been characterized by powder X-ray diffraction in the temperature interval studied. A revised version or the copper-rich part or the phase diagram is presented. All transitions are characterized by hysteresis in the attainment of equilibrium and a greater or lesser dependence on thermal history and/or thermal recycling. Thermodynamic functions have been evaluated and selected values are shown in Table 4.

Table 4
Selected values of evaluated thermodynamic functions.

	$C_{p,m}/R$	$\Delta^{T}_{0}S^{o}_{m}/R$	ϕ^{o}_{m}/R	T/K
(1/2.90)$Cu_{1.90}S$	(3.166)	4.654	2.5148	298.15
	3.478	8.080	4.9280	700
(1/2.92)$Cu_{1.95}S$	3.109	4.679	2.5353	298.15
	3.446	8.145	4.9391	700
	3.420	9.361	6.0945	1000
	$C_{p,m}/R$	$\Delta_{T298.15K}S^{o}_{m}/R$	$\Delta_{T298.15K}H^{o}_{m}/(R\cdot K)$	T/K
(1/2.98)$Cu_{1.98}S$	3.042	0	0	298.15
	3.395	3.529	1643.4	700
	3.384	4.723	2546.9	1000
(1/2.995)$Cu_{1.995}S$	3.027	0	0	298.15
	(4.02)	3.564	1660.7	700

An associated solution model is applied in [41] to describe the thermodynamic behavior of Cu-S as a liquid. This model assumes the existence of 'Cu_2S' species in addition to Cu and S in the liquid. With two solution parameters for each of the binaries Cu-'Cu_2S' and 'Cu_2S'-S, this model accounts for the compositional dependence of the thermodynamic properties of Cu-S liquid from pure Cu to pure S over a wide range of temperature. The binary Cu-S does not contribute significantly to the excess Gibbs energy of the liquid due to the rather small dissociation constant of 'Cu_2S' to Cu and S. Using this model for the liquid phase, a statistical thermodynamic model for the digenite phase, and appropriate thermodynamic equations for the other phases, the Cu-S phase diagram is calculated. The calculated diagram is in excellent agreement with the experimental data, accounting for the range of homogeneity of digenite at all temperatures.

The thermodynamic properties of the CuS - Cu_2S system have been studied in [42] by means of adiabatic-shield calorimetry in the temperature range 5 to 1000 K. The heat-capacity curves show the presence of a large number of transitions which have been characterized structurally by powder X-ray and neutron diffraction. A revised phase diagram is presented. The heat-capacity data serve as a starting point for evaluation and discussion of the thermodynamic proper-

ties of the CuS - Cu_2S system. The calorimeter used for the high-temperature measurements and the experimental procedure are described in some detail.

In [43] the phase diagram was investigated and thermodynamic data for all copper sulfide phases in the system Cu-S was determined with electrochemical methods. The temperature interval was 15-90°C.

The following observations were made in [44]. In a wide range of temperatures, the specific heats of the cubic phases of cuprous sulfide and cuprous selenide increase with increasing copper deficit δ, if the specific heats are referred to the formula $Cu_{2-\delta}X$ (X = S,Se). In other words, the partial specific heats of copper are negative. Just above the phase transformation tetragonal cubic, cuprous selenide was found to have partial specific heats of copper which do not deviate much from Dulong-Petit's value. But, with increasing temperature Cp_{Cu} decreases and approaches a minimum value of negative sign around 450°C. An interpretation of this finding is proposed. Furthermore, with the measurements of this work the phase diagrams Cu_2X-CuX could be extended.

The heat capacities of $Cu_{1.75}S$, $Cu_{1.80}S$, and $Cu_{1.85}S$ have been measured in [45] by adiabatic-shield calorimetry from 5 to about 700 K. The heat-capacity curves show transitions near 312, 337, and 355 K in $Cu_{1.75}S$ and $Cu_{1.80}S$ and near 312, 368, and 376 K in $Cu_{1.85}S$. This implies a revision of existing phase diagrams. All transitions are characterized by hysteresis in the attainment of equilibrium and a greater or lesser dependence on thermal history and/or thermal recycling. Thermodynamic functions have been evaluated and selected values are shown in Table 5.

Table 5
Selected values of evaluated thermodynamic functions.

	Cop,m/R	$\Delta^T{}_oS^o{}_m(T)/R$	$\phi^o{}_m(T,o)/R$	T/K
$(1/2.75)Cu_{1.75}S$	3.354	4.702	2.526	298.15
	3.571	8.104	4.977	700
$(1/2.80)Cu_{1.80}S$	3.614	4.708	2.527	298.15
	3.541	8.129	4.994	700
$(1/2.85)Cu_{1.85}S$	3.246	4.650	2.497	298.15
	3.476	8.085	4.945	700

5.2 Phase diagrams

In [46], the copper-sulfur phase diagram has been drawn from 20°C to 500°C. In the compositional region $Cu_{2.00}S$-$Cu_{1.96}S$ studies were performed by the isothermal variations of the electromotive force of a solid copper-copper bromide-copper sulfide cell against the deviation from stoichiometry and by the thermal

variations of electronic properties. The discontinuity of the curves are interpreted as the phase transitions of the sample. In the region of very weak deviations from stoichiometry the copper-rich limit of the existence range of copper sulfide has been drawn from the study of the solid cell and from the measures of the Hall effect made in the orthorhombic chalcocite range.

X-ray diffraction data collected on a single crystal specimen of CuS_2 show that despite its optical anisotropy CuS_2 apparently has the cubic pyrite structure, with a = 5.7891(6) Å [47]. Precession and Weissenberg photographs fail to reveal any reflections which violate the requirements for space group Pa3. Such reflections, however, were observed in four-circle diffractometer measurements, but they are shown to result from multiple diffraction effects. Refinement of the structure in space group Pa3 using 209 intensity data gives a weighted residual of 0.014 and x(S) = 0.39878(5). A comparison of the refined structure with other pyrite structures suggests that copper in CuS_2 has a formal valence of 2+ and three antibonding electrons. Also, the CuS_6 octahedron is only slightly distorted, which is in contrast with the square-planar coordination usually found for Cu^{2+}.

The system CuAgS is investigated [48]. This system is characterized by several phases with highly disordered cation sites, extensive solid solutions, and reaction rates so rapid as to be unquenchable. Ternary compounds, occurring only along the join Cu_2S-Ag_2S, are jalpaite ($Cu_{0.45}Ag_{1.55}S$), stromeyerite ($Cu_{1+x}Ag_{1-x}S$) and $Cu_{0.8}Ag_{1.2}S$. Although orthorhombic chalcocite (Cu_2S) can dissolve up to 1.87 + 0.37 mol % Ag_2S at 63° C, at high temperatures a cation-disordered, nonquenchable solid solution with a hexagonal closest packed (hcp) structure exists from Cu_2S to $(Cu_{0.96}Ag_{1.04})S$. Chalcocite becomes hexagonal at 103.5° C and stromeyerite inverts to the same hcp structure at 93.3° C. The eutectoid between chalcocite and stromeyerite is at $(Cu_{1.76}Ag_{0.24})S$ and 67° C. $Cu_{0.8}Ag_{1.2}S$ breaks down at 94.4° C to jalpaite + $(Cu_{0.96}Ag_{1.04})S$. Jalpaite inverts at 117° C to a copper rich argentite with a body centered cubic (bcc) structure. At 420° C and 593° C, respectively, Cu_2S and Ag_2S invert to face centered cubic (fcc) phases with structures identical to that of "highdigenite." The fcc phase has a lowest temperature of stability of 115° C at a composition of $(Cu_{0.88}Ag_{1.12})S$. Above this temperature the field expands across the Cu_2S-Ag_2S join and also towards more sulfur rich compositions, replacing all other phases including digenite. After the inversion of sulfur rich argentite at 622° C, a broad fcc field extends as a belt across the ternary diagram. Examination of assemblages with bulk compositions in the system Cu-Ag-S indicates that in nature, as in the laboratory, reaction rates are rapid. The former existence of high temperature phases has been demonstrated by the preservation of pseudomorphs and can be inferred from certain textural evidence.

5.3 Some important observations

- Data on $\Delta fG^{\circ}m$, $\Delta fH^{\circ}m$ and $\Delta fS^{\circ}m$ for Ag_2S and CuS is accounted.

- Potential pH-diagrams for the systems Cu-H_2O, Fe-H_2O and Fe-Cu-H_2O systems are presented and the solubilities of copper and iron oxides (including mixed copper-iron oxide) are evaluated.

- Thermochemical data are used to construct a modified log-activity diagram for the system Cu-H-O-Cl-(CO_2).

- Heat capacities of $Cu_{1.90}S$, $Cu_{1.95}S$, $Cu_{1.98}S$ and $Cu_{1.995}S$ are measured by adiabatic-shield calorimetry and all samples have been characterized by powder X-ray diffraction in the temperature interval studied. A revised version or the copper-rich part or the phase diagram is presented.

- The thermodynamic properties of the CuS - Cu_2S system have been studied by means of adiabatic-shield calorimetry in the temperature range 5 to 1000 K. The heat-capacity curves show the presence of a large number of transitions which have been characterized structurally by powder X-ray and neutron diffraction. A revised phase diagram is presented.

- In a wide range of temperature, the specific heats of the cubic phases of cuprous sulfide and cuprous selenide increase with increasing copper deficit δ, if the specific heats are referred to the formula $Cu_{2-\delta}X$ (X = S,Se). With increasing temperature, Cp_{Cu} decreases and approaches a minimum value of negative sign around 450°C.

- Heat capacities of $Cu_{1.75}S$, $Cul_{1.80}S$, and $Cu_{1.85}S$ have been measured by adiabatic-shield calorimetry from 5 to about 700 K. The heat-capacity curves show transitions near 312, 337, and 355 K in $Cu_{1.75}S$ and $Cu_{1.80}S$. and near 312, 368, and 376 K in $Cu_{1.85}S$. This implies a revision of existing phase diagrams.

- The copper-sulfur phase diagram is drawn from 20 °C to 500 °C, in the compositional region $Cu_{2.00}S$-$Cu_{1.96}S$.

- X-ray diffraction data collected on a single crystal specimen of CuS_2 show that despite its optical anisotropy CuS_2 apparently has the cubic pyrite structure, with a = 5.7891(6)Å. The CuS_6 octahedron is only slightly distorted, which is in contrast with the square-planar coordination usually found for Cu^{2+}.

- The system CuAgS is characterized by several phases with highly disordered cation sites, extensive solid solutions, and reaction rates so rapid as to be unquenchable.

6 Structure

The crystal structure of Ag_3CuS_2 has been determined in [49] by using X-ray powder diffraction data. The unit cell is tetragonal, a = 8.6705(10), c = 11.7573(18) Å, and the space group is $I4_1/amd$ (141) with Z=8. A starting model for the structure was derived by using direct methods and difference Fourier cycling from 93 unambiguously indexed integrated intensities, and then refined by the Rietveld method. Both diffractometer and Guinier-Hägg data were utilized. Corroborative evidence for the correctness of the resulting structure was obtained by comparison of experimental and calculated single-crystal electron diffraction intensities.

The Ag_3CuS_2 structure is based on distorted bcc sulfur packing. There are two distinct silver sites. In one the silver atom is surrounded by six sulfur atoms forming a [2+4] distorted octahedral environment. In the other site the silver atom is in a distorted tetrahedral environment with two sulfur atoms nearby and two more, somewhat farther away. Copper is linearly coordinated by two sulfur atoms.

7 Leaching

The leaching behavior of copper from natural chalcocite (Cu_2S) particles in alkaline Na_4EDTA solutions containing oxygen was examined in [50] at atmospheric pressure. The EDTA leaching process took place with consecutive reactions, where the solid product of the first reaction, covellite (CuS), became the reactant for the second. The copper leached into the alkaline solutions was immediately consumed by the chelation of copper (II) with EDTA, and the mineral sulfur was completely oxidized to sulfate ion. The experimental data for the leaching rate of copper were analyzed with a familiar shrinking-particle model for reaction control. The conversion rate of chalcocite to covellite was found to be about 10 times as high as the dissolution rate of covellite. The time required for complete dissolution of covellite was directly proportional to the initial particle size and was inversely proportional to the square root of the product of the hydroxide ion concentration and the oxygen partial pressure, but it was independent of the Na_4EDTA concentration in the presence of excess Na_4EDTA. The observed effects of the relevant operating variables on the dissolution rate were consistent with a kinetic model for electrochemical reaction control. The kinetic model was developed by applying the Butler-Volmer equation to the electrochemical process, in which the anodic reaction involves the oxidation of covellite to copper (II) ion and sulfate ion and the cathodic reaction involves the reduction of oxygen in alkaline solution. The rate equation allowed us to predict the time required for the complete leaching of copper from chalcocite in the alkaline Na_4EDTA solutions.

8 Kinetics

It is claimed in [51] that measured concentrations of redox couples in low temperature, aerated ground waters often yield conflicting potentials, making it difficult to define system-wide redox conditions for use in equilibrium geochemical models. Redox desequilibrium is caused, in part, by the slow rates at which the reduced species are oxidized by dissolved O_2. To describe these rates, literature data were used to calculate half lives for the ΣFe^{2+}, ΣS^{2-}, ΣCu^{+}, and ΣMn^{2+} oxygenation reactions as a function of pH at 0.2 atm O_2. These data and experimentally measured rates for ΣAs^{3+} oxygenation yield half-lives in the range from seconds to years, depending on solution conditions. The large differences in half-lives, which are strongly dependent on pH, imply that some reduced species are rapidly oxidized, whereas others may metastabely persist in oxidizing environments, resulting in redox disequilibrium. The half-life versus pH diagrams provide a convenient means for comparing oxygenation rates and assessing likely conditions for disequilibrium between reduced species and the $O_2(aq)/H_2O$ couple.

9 Conductivity

It is claimed in [52], that in a contaminated atmosphere, contact resistance increase is generally attributed to corrosion film growth. Its usual measurement does not reveal basic conduction phenomenon which occur at the contact point. In this report results are accounted concerning electrical conduction through the main Cu_2S film grown on copper samples in a reaction chamber (10 ppm of H_2S). The study is based on the analysis of current-voltage (I-V) characteristics of the contact point, by using a fully automatic device which avoids electrical or mechanical breakdowns. It is demonstrated that the contact point has an equivalent circuit composed of serial elements: diode, thermoelectric voltage, and contact resistance. Tbe diode parameters resulting from the junction between Cu_2S (semiconductor) and copper (metal) are determined. The main result is the relationship between reverse current density and the thickness of the film (100 to 5000 Å) which can explain and predict film breakdown. Furthermore, dynamic contact resistance depends on current level and direction; its limit (static resistance) is reached with higher current level values or with gilded film.

10 Pitting corrosion

In [53] the electrochemical behavior of copper electrodes in NaOH solutions with the addition of Na_2S was studied through the analysis of current transients under constant potential and complementary voltametric and scanning electron microscopy data including energy dispersive X-ray analysis. The overall process can be described by the following three stages. The first stage corresponds to the nucleation and growth of a complex copper sulfide layer at potential values close to the equilibrium potentials of the Cu/Cu_2S and Cu/CuS reversible electrodes. The second stage is related to the rupture of the copper sulfide film at potentials more positive than a certain critical value leading to pitting corrosion of copper metal and yielding a poorly protective copper sulfide layer. The third stage occurs in the copper oxide electroformation range, where the presence of copper sulfide accelerates the electrodissolution of the base metal and copper oxide hinders the sulfidization processes. The current transients of each stage are interpreted through a model based on the nucleation and growth mechanism.

11 Other heavy metals

From archaeological finds it has been observed and reported in [54] that grain size and shape is the factor governing the corrosion durability of lead. For long term corrosion stability, the grain size should not exceed 0.5 mm grain diameter. On the basis of an investigation of 2000 year old artefacts, conclusions are drawn and manufacturing conditions for lead containers for the burial of high-level atomic waste are recommended.

In [55], copper and copper-iron sulfides can be classified into three general groups: (1) anilite, digenite, geerite, cubanite, chalcopyrite, haycockite, talnakhite, mooihoekite and bornite with structures based upon approximate cubic closepacking of the sulfur atoms; (2) djurleite and chalcocite with structures based upon approximate hexagonal closepacking of the sulfur atoms; (3) covelline, yarrowite, spionkopite and idaite with a combination of hexagonal close packing and covalent bonding of the sulfur atoms. The average spacing D between layers in all groups can be expressed as $D = 2.063 + 0.654$ (Cu:S) + 1 .183 (Fe:S). For group-2 minerals, $R \approx 1.856 + 0.060$ (Cu:S) + 0.023 (Fe:S). For group-3 minerals, RI = 1.857 + 0.039 (Cu:S) 0.020 (Fe:S). Consideration of bond lengths in coordination polyhedra of known copper sulfide structures indicates that major portions of the yarroite and spionkopite structures will resemble the covelline structure, with probable statistical site occupancy. Attempts at the determination of the spionkopite structure were hampered by the imperfection of the crystals and the partial occupancy of most structural positions of copper. The geerite structure is rhombohedral (R3m?) with a 15.77 A, ~ 13°56', Z= 1, and will probably resemble the digenite structure.

It is claimed in [56] that nothing has earlier been published on fusion in the Cu_2S-FeS-Na_2S-PbS system; only the binary and ternary system which form the edges and faces of the concentration tetrahedron of this quaternary system have been studied and their equilibrium diagrams constructed.

The composition found for the copper-rich double compound in the Cu_2S-Na_2S system by Kopylov and Novoselov was not confirmed later by Kopylov, therefore the results on the Cu_2S-Na_2S-PbS system were corrected in accordance with Kopylov's results.

References

1 CHEN, Q et al
Kinetics of Desulfurization of Hydrogen Sulfide Using Metallic Copper as Desulfurizer.
Can J Chem Eng 69 (Oct 1991), 1160-1165.

2 COURTY, C et al
Tarnishing of Au-Ag-Cu Alloy Studied by Auger Electron Spectroscopy and Coulometry.

3 FIAUD, C and GUINEMENT, J
The Effect of Nitrogen Dioxide and Chlorine on the Tarnishing of Copper and Silver in the Presence of Hydrogen Sulfide.
Symp Corrosion Effects of Acid Deposition, Las Vegas 1985, 280-304.

4 PAYER, J H and CHAWLA, S K
Tarnishing of Copper in Moist Air Containing Trace Levels of Sulfur Dioxide.
Elchem Soc Fall Meeting 15-20 Oct, 1989. Extended Abstract #143, p 208.

5 FIAUD, C et al
Identification of the Corrosion Products Formed on Copper in Sulfur Containing Environments.
Werkstoffe und Korrosion 35, 361-366 (1984).

6 DANKO, V A et al
Photodoping in the As_2S_3 - Ag Thin Film Structure.
Phys Stat Sol (a) 124, 235 (1991).

7 SUZUKI, M and KOYAMA, H
Analysis of Atmospheric Corrosion Products of Copper.
Jitsumu Hyöomen Gijutsu 24 (1973):12, pp 668-73.

8 BARTKOWICZ, I and STOKLOSA, A
Kinetics of Copper Sulfidation at Temperatures 570-1123 K.
Oxidation of Metals, Vol. 25, Nos. 5/6, 1986.

9 DHUMURE, S S and LOKHANDE, C D
Preparation and Characterization of Chemically Deposited Ag_2S Films.
Solar Energy Materials and Solar cells 28(1992) 159-166.

10 HELZ, G and HORZEMPA, L M
EDTA as a Kinetic Inhibitor of Copper (II) Sulfide Precipitation.
Water Res, Vol 17, pp167 to 172, 1983.

11 AL HAJJI, J N and REDA, M R
The Corrosion of Copper-Nickel Alloys in Sulfide-Polluted Seawater: The effect of Sulfide Concentration.
Corrosion Science, Vol 34, No 1, pp 163-177, 1993.

12 SHEA, D and HELZ, G R
Kinetics of Inhibited Crystal Growth: Precipitation of CuS from Solutions Containing Chelated Copper(ll).
Journal of Colloid and Interface Science Vol 116, No.2, April 1987.

13 POTTER, R
An Electrochemical Investigation of the System Copper-Sulfur.
Economic Geology Vol 72.1, 1977, pp 1524-1542.

14 EVANS, H
Djurleite ($Cu_{1.9}4S$) and Low Chalcocite (Cu_2S):
New Crystal Structure Studies.
Science Vol 203, 26 Jan 1979, pp 356-358.

15 EVANS, H T
The Crystal Structures of Low Chalcocite and Djurleite.
Zeitschrift für Kristallographie 150, 299-320 (1979).

16 KOPYLOV, N I et al
The Cu_2S-FeO System.
Russian Journal of Inorganic Chemistry 37(12) 1992.

17 McNEIL, M B et al
Production of Sulfide Minerals by Sulfate-Reducing Bacteria During Microbiologically Influenced Corrosion of Copper.
Corrosion. NACE, Sep 1991, 47(91), pp 674-677.

18 YAMAMOTO, K and KASHIDA, S
X-Ray Study of the Average Structures of Cu_2Se and $Cu_{1.8}S$ in the Room Temperature and the high Temperature Phases.
J Solid State Chemistry 93, 202-211 (1991).

19 MORIMOTO, J and MIYAKAWA, T
Diffusion of Cu in Cu.S-CdS Heterojunction Diodes
Memoirs of the National Defence Academy, Japan,vol 27, No 3-4 (1987), pp 97-107.

20 KOPYLOV, N et al
Phase Diagram of the Cuprous Sulfide-Ferrous Sulfide-Ferrous Oxide System.
Tsvetn Met (Moscow), 5, 22-24 (1992).

21 RICKERT, H and WIEMHÖFER, H-D
Measurements of Chemical Diffusion Coefficients of Mixed Conducting Solids Using Point Electrodes - Investigations on Cu_2S.
Solid State Ionics 11 (1983), 257-268.

22 BUTRYMOWICZ, D B et al
Diffusion in Copper and Copper Alloys.
Part II. Copper-Silver and Copper-Gold Systems
J Phys Chem Ref Data Vol 3, No 2, 1974, pp 527-602.

23 TINTER, U and WIEMHÖFER, H-D
Chemical Diffusion Coefficients of Low Temperature Phases of Cu_xSe and Cu_xS. Investigations with Point Electrodes.
Solid State Ionics 9 & 10 (1983), p 1213-1220.

24 BENTE, K and DOERING
Solid-State Diffusion in Sphalerites: an Experimental Verification of the "Chalcopyrite Disease".
Eur J Mineral 1993, 5, 465-478.

25 YAMAMOTO, K and KASHIDA, S
X-Ray Study of the Average Structures of Cu_2Se and $Cu_{1.8}S$ in the Room Temperature and the High Temperature Phases.
J Solid State Chemistry, 93, 202-211 (1991).

26 CAVA, R J et al
Mobile Ion Distribution and Anharmonic Thermal Motion in Fast Ion Conducting Cu_2S.
Solid State Ionics 5 (1981) 501-504.

27 YAMAMOTO, K and KASHIDA, S
X-Ray Study ofthe Cation Distribution in Cu_2Se, $Cu_{1.8}Se$ and $Cu_{1.8}S$; analysis by the maximum entropy method.
Solid State Ionics 48 (1991) 241-248.

28 HSIEH, H C.
The Effect of Cu Diffusion in a Cu_2S/Cds Heterojunction Solar Cell.
J Appl Phys 53(3), March 1982, pp 1727-1733.

29 RASTOGI, A C and SALAKALCHEN, S
X-Ray Photoelectron Spectroscopy Studies of Copper Diffusion Behavior and Related Degradation Phenomena in Thin Film CdS-Cu_2S Solar Cells.
Solar Cells, 9 (1983), 185-202.

30 RENDERS, P J and SEWARD, T M
The Stability of Hydrosulphido- and Sulphido-complexes of Au(I) and Ag(I) at 25 °C.
Geochim Cosmochim Acta 53 (1989), 245-253.

31 GAMMONS, C H and BARNES, H L
The Solubility of Ag_2S in Near-Neutral Aqueous Sulfide Solutions at 25 to 300 °C.
Geochim Cosmochim Acta, 53(1989), 279 - 290.

32 SHEA, D and HELZ, G R
Solubility Product Constants of Covellite and Poorly Crystalline Copper Sulfide Precipitate at 298 K.
Geochim Cosmochim Acta, 53(1989), 229 - 236.

33 DUDA, L and BARTECKI, A
Dissolution of Cu_2S in Aqueous EDTA Solutions Containing Oxygen.
Hydrometallurgy, 8 (1982), 341-354.

34 GRIZO, A et al
Leaching of a Low-Grade Chalcocite-Covellite Ore Containing Iron in Sulfuric Acid;The Influence of pH and Particle Size on the Kinetics of Copper Leaching.
Hydrometallurgy, 8 (1982).

35 WOLINSKI, W K and MILLER, J D A
A Rotating Disc Electrode Giving Reproducible Electrochemical Leaching Kinetics for Copper Sulphide.
Laboratory Practice, January 1983, pp 60-62.

36 CATTARIN, S and TRIBUTSCH, H
Interfacial Reactivity and Oscillating Behavior of Chalcopyrite Cathodes during H_2O_2 Reduction. I. Electrochemical Phenomena.
J Electrochem Soc, Vol 137, No 11, Nov 1990, 3475-3483.

37 SAGUA, A E
On the Phase Equilibrium of (Ag2S+S) and (CuS+S) from emf Measurements in Solid State Galvanic Cells.
Mat Chem Pys, 32(1992), 235-239.

38 CUBICCIOTTI, D
Pourbaix Diagrams for Mixed Metal Oxides: The Chemistry of Copper in BWR Water.
Corrosion 88(1988) paper 254.

39 MOHR, D W and McNEIL, M B
Modified log-activity Diagrams as a Tool for Modelling Corrosion of Nuclear Waste Container Materials, with Particular Reference to Copper.
J Nucl Mat, 190(1992), 329 - 342.

40 STÖLEN, S et al
Thermodynamics of Copper Sulfides.
IV. Heat Capacity and Thermodynamic Properties of $Cu_{1.90}S$ from 5 K to 750 K, $Cu_{1.95}S$ from 5 K to 1000 K, $Cu_{1.98}S$ from 300 K to 1000 K, and $Cu_{1.995}S$ from 300 K to 750 K.
J. Chem. Thermodynamics 1990, 22, 1035-1057.

41 SHARMA, R C and CHANG, Y A
A Thermodynamic Analysis of the Copper-Sulfur System.
Met Trans B (AIME), Vol 11B, Dec 1980.

42 STÖLEN, S and GRÖNVOLD, F
Thermodynamic Properties of the CuS - Cu_2S System.
Thermochemistry of Alloys, 213-220. H. Brodowsky and H-J Schaller (eds). (c) 1989 by Kluwer Academic Publishers.

43 MATHIEU, H J and RICKERT, H
Elektrochemisch-Thermodynamische Untersuchungen am System Kupfer--Schwefel bei Temperaturen T = 15-90 °C.
Z Phys Chem Neue Folge, Bd. 79, s 315-330 (1972).

44 KUBASCHEWSKI, P.
Spezifische Wärmen und thermische Fehlordnung von Kupferchalkogeniden.
Teil II: Die Systeme Cu_2S-Cus und Cu_2Se-CuSe
Berichte der Bunsengesellschaft, Phys Chem 77 (1973).

45 GRÖNVOLD, F et al
Thermodynamics of Copper Sulfides.
Heat Capacities and Thermodynamic Properties of $Cu_{1.75}S$ $Cu_{1.80}S$ and $Cu_{1.85}S$ from 5 to about 700 K.
J Chem Thermodynamics 1987, 19, 1305-1324.

46 DUMON, P A et al
Étude du Diagramme des Phases du Système CuS dans L´intervalle de Composition $Cu_{2.000}S$ - $Cu_{1.960}S$.
J Chimie Phys 1974, 71 No3, pp 407-414.

47 KING, H E and PREWITT, C T
Structure and Symmetry of CuS_2 (Pyrite Structure).
American Mineralogist, Vol 64, pp 1265-1271, 1979.

48 SKINNER, B J
The System Cu-Ag-S.
Econ Geol Vol 61(1), Jan - Feb, 1966.

49 BAKER, C L et al
Crystal Structure Determination of Ag_3CuS_2 from Powder X-Ray Diffraction Data.
Aust J Chem, 1992, 45, 1441-1449.

50 KONISHI, Y et al
Leaching Kinetics of Copper from Natural Chalcocite in Alkaline Na_4EDTA Solutions
Met Trans B vol 22B, June 1991, 295-303.

51 EARY, E L and SCHRAMKE, J A
Rates of Inorganic Reactions Involving Dissolved Oxygen.
Am Cer Soc Symp 1990, 379 - 397.

52 BEN JEMAA, N et al
Electrical Conduction Through Cu_2S Corrosion Films on Copper Contacts.
IEEE Trans on Components, Hybrids and Manufact Tech, Vol 13(4), Dec 1990, 1063-1067.

53 VASQUES MOLL, D et al
Corrosion and Passivity of Copper in Solutions Containing Sodium Sulfide. Analysis of Potentiostatic Current Transients
Electrochimica Acta Vol 30, No 8, pp 1011-1016, 1985.

54 KRYSKO, W W
Blei als Behälterwerkstoff für Atommüll.
Analyse des Korrosionsverhaltens aufgrund archäologischer Funde.
Metallwissenschaft und Technik, Metall 34. Jahrgang, Heft 5, Mai 1980.

55 GOBLE, R
The Relationship between Crystal Structure, Bonding and Cell Dimensions in the Copper Sulfides.
Canadian Mineralogist Vol 23, pp 61-76 (1985).

56 KOPYLOV, N I
The Cu_2S-FeS-Na_2S-PbS System.
Russian Journal of Inorganic Chemistry, 14 (6), 1969.

STATENS KÄRNKRAFTINSPEKTION
Swedish Nuclear Power Inspectorate

Postadress/Postal address	Telefon/Telephone	Telefax	Telex
SKI S-106 58 STOCKHOLM	Nat 08-698 84 00 Int +46 8 698 84 00	Nat 08-661 90 86 Int +46 8 661 90 86	11961 SWEATOM S